



HAL
open science

Bioinspired hyaluronic acid and polyarginine nanoparticles for DACHPt delivery

Kevin Matha, Giovanna Lollo, Giuseppe Taurino, Renaud Respaud, Ilaria Marigo, Molood Shariati, Ovidio Bussolati, An Vermeulen, Katrien Remaut, Jean-Pierre Benoît

► **To cite this version:**

Kevin Matha, Giovanna Lollo, Giuseppe Taurino, Renaud Respaud, Ilaria Marigo, et al.. Bioinspired hyaluronic acid and polyarginine nanoparticles for DACHPt delivery. *European Journal of Pharmaceutics and Biopharmaceutics*, 2020, 150, pp.1-13. 10.1016/j.ejpb.2020.02.008 . hal-02496238

HAL Id: hal-02496238

<https://hal.science/hal-02496238>

Submitted on 5 Mar 2020

HAL is a multi-disciplinary open access archive for the deposit and dissemination of scientific research documents, whether they are published or not. The documents may come from teaching and research institutions in France or abroad, or from public or private research centers.

L'archive ouverte pluridisciplinaire **HAL**, est destinée au dépôt et à la diffusion de documents scientifiques de niveau recherche, publiés ou non, émanant des établissements d'enseignement et de recherche français ou étrangers, des laboratoires publics ou privés.

Bioinspired hyaluronic acid and polyarginine nanoparticles for DACHPt delivery

Authors : [Kevin Matha](#)^{a,b}, Giovanna Lollo^c, Giuseppe Taurino^d, Renaud Respaud^{e,f}, Ilaria Marigo^g, Molood Shariati^h, Ovidio Bussolati^d, An Vermeulenⁱ, Katrien Remaut^h, and Jean-Pierre Benoit^{a,b}.

a. Micro et Nanomédecines Translationnelles, MINT, UNIV Angers, UMR INSERM 1066, UMR CNRS 6021, Angers, France

b. CHU Angers, département Pharmacie, 4 rue Larrey, 49933 Angers cedex 9.

c. Univ Lyon, Université Lyon 1, CNRS, UMR 5007, Laboratoire d'Automatique, de Génie des Procédés et de Génie Pharmaceutique (LAGEPP), 43 bd du 11 Novembre 1918, F-69622 Lyon, France.

d. Department of Biomedical, Biotechnological, and Translational Sciences, University of Parma, 43100 Parma, Italy.

e. Centre d'Étude des Pathologies Respiratoires-CEPR, Institut National de la Santé et de la Recherche Médicale-INSERM, Unité Mixte de Recherche UMR1100, Labex Mabimprove, 37000 Tours, France.

f. Centre Hospitalier Régional Universitaire-CHRU de Tours, Hôpital Trousseau, Service de Pharmacie, 37170 Chambray-les-Tours, France.

g. Istituto Oncologico Veneto, IOV-IRCCS, 35128 Padova, Italy.

h. Ghent Research Group on Nanomedicines, Laboratory of General Biochemistry and Physical Pharmacy, Faculty of Pharmaceutical Sciences, Ghent University, Ghent, Belgium.

i. Laboratory of Medical Biochemistry and Clinical Analysis, Faculty of Pharmaceutical Sciences, Ghent University, Ottergemsesteenweg 460, B-9000, Ghent, Belgium.

Corresponding author: jean-pierre.benoit@univ-angers.fr

Keywords: DACHPt, Hyaluronic acid, Polyarginine, Polymeric Nanoparticles, Anticancer treatment

Published in European Journal of Pharmaceutics and Biopharmaceutics 2020 Feb 27[Online ahead of print]

DOI: [10.1016/j.ejpb.2020.02.008](https://doi.org/10.1016/j.ejpb.2020.02.008)

PMID: **32113915**

https://pubmed.ncbi.nlm.nih.gov.proxy.insermbiblio.inist.fr/32113915-bioinspired-hyaluronic-acid-and-polyarginine-nanoparticles-for-dachpt-delivery/?from_single_result=10.1016%2Fj.ejpb.2020.02.008

Abstract

This work provides insights over a novel biodegradable polymeric nanosystem made of hyaluronic acid and polyarginine for diaminocyclohexane-platinum (DACHPt) encapsulation. Using mild conditions based on ionic gelation technique, monodispersed blank and DACHPt-loaded nanoparticles with a size of around 200 nm and negative ζ potential (-35 mV) were obtained. The freeze-drying process was optimized to improve the stability and shelf-life of the developed nanoparticles. After reconstitution, nanoparticles maintained their size showing an association efficiency of around 70 % and a high loading efficacy (8%). *In vitro* cytotoxicity studies revealed that DACHPt-loaded nanoparticles had a superior anticancer activity compared with oxaliplatin solution. The IC₅₀ was reduced by a factor of two in HT-29 cells (IC₅₀ 39 μ M vs 74 μ M, respectively), and resulted almost 1.3 fold lower in B6KPC3 cells (18 μ M vs 23 μ M respectively). Whereas toxic effects of both drug-formulations were comparable in the A549 cell line (IC₅₀ 11 μ M vs 12 μ M). DACHPt-loaded nanoparticles were also able to modulate immunogenic cell death (ICD) *in vitro*. After incubation with B6KPC3 cells, an increase in HMGB1 (high-mobility group box 1) production associated with ATP release occurred. Then, *in vivo* pharmacokinetic studies were performed after intravenous injection (IV) of DACHPt-loaded nanoparticles and oxaliplatin solution in healthy mice (35.9 μ g of platinum equivalent/mouse). An AUC six times higher (24 h*mg/L) than the value obtained following the administration of oxaliplatin solution (3.76 h*mg/L) was found. C_{max} was almost five times higher than the control (11.4 mg/L for NP vs 2.48 mg/L). Moreover, the reduction in volume of distribution and clearance clearly indicated a more limited tissue distribution. A simulated repeated IV regimen was performed *in silico* and showed no accumulation of platinum from the nanoparticles. Overall, the proposed approach discloses a novel nano-oncological treatment based on platinum derivative with improved antitumor activity *in vitro* and *in vivo* stability as compared to the free drug.

Introduction

Platinum-based antitumor agents are among the most widely used anticancer drugs for treatment of lung, colorectal, ovarian, head and neck, breast, and bladder cancers [1,2]. Cisplatin, the first compound approved by the US Food and Drug Administration (FDA) [3] in 1979, had a profound impact on cancer management and is now commonly used in medical oncology. However, serious concerns due to resistance phenomena and dose limiting toxicity hamper its clinic use. To overcome these limitations, significant efforts have been devoted to develop novel analogues with a better toxicity profile and improved activity. Modification including the replacement with an oxalate ligand as leaving group and the diaminocyclohexane (DACH) ligand in the trans-L isomer led to the design of oxaliplatin (trans-L-diaminocyclohexane oxalate platinum (II)). Oxaliplatin is a prominent third-generation drug that retains the antitumor properties of cisplatin without its clinical toxicity profile [4]. In addition to DNA damage, oxaliplatin induces ribosome biogenesis stress [5] and helps generating immune response against tumors by triggering the immunogenic cell death (ICD) [6,7].

Despite these positive features in terms of efficacy, neurotoxicity with repeated cycles of oxaliplatin administration [8] and cases of renal failure have been reported [9,10].

In this context, nanomedicines hold great promise to improve platinum-based anticancer treatments by reducing drug toxicity and enhancing therapeutic efficacy by tissue- or cell- targeting. So far, many efforts have been made to develop nanocarriers entrapping oxaliplatin or its derivatives [1,11–15]. The encapsulation of platinum-based drugs in liposomes showed an improved anticancer activity on several tumor models in comparison with non-encapsulated drug [16]. MBP-426, a liposomal formulation carrying oxaliplatin and decorated with transferrin, is currently in Phase II clinical development in combination with leucovorin and 5-fluorouracil for the treatment of gastric adenocarcinoma [17]. Polymeric nanoparticles (NP) and micelles were also investigated for platinum delivery. AP5346 (ProLindac®, Access Pharmaceuticals, Inc.), NP made of N-(2-hydroxypropyl)methacrylamide (HPMA) conjugated to DACHPt [18] showed a superior activity in terms of tumor growth inhibition and safety profile [19]. Despite the improvement of its anticancer activity, the

system described above presented some concerns regarding the need for chemical synthesis during the formulation process, low loading efficiency and rapid leakage of the drug during storage. Cabral and colleagues developed a co-polymeric micelle composed of PEG-b-(poly)glutamic acid for cisplatin or (1,2-diaminocyclohexane)platinum(II) (DACHPt) encapsulation [20,21]. DACHPt micelles exhibited remarkably prolonged blood circulation and greater accumulation in tumor tissue compared to free oxaliplatin [20]. Based on this background, the aim of the present work has been to design and develop a novel NP-based system made of bioinspired polymers such as hyaluronic acid (HA) and polyarginine (PA) for DACHPt encapsulation [22]. HA and PA have been chosen due to their non-toxicity, biodegradability and biocompatibility profile [23]. HA is an anionic polysaccharide widely used in biomedical applications [24–26]. It is a glycosaminoglycan and an important component of the extracellular matrix (ECM). Moreover, it can specifically recognize membrane glycoproteins such as CD44 receptors overexpressed by various cancer cells [27,28]. PA is a cationic polyaminoacid consisting in the repetition of 28 to 32 arginine moieties, that can be degraded by peptidases in the body ensuring high biocompatibility. DACHPt-loaded NP were optimized, physico-chemically characterized and their cytotoxic activity was assessed *in vitro* against pancreatic (B6KPC3), lung (A549) and colon (HT-29) cancer cells lines. The ability of DACHPt-loaded NP to induce ICD by quantifying release of alarmins such as HMGB1 (High-mobility group box 1) and ATP were also evaluated. The uptake mechanism of these nanosystems by cancer cells was also evaluated in correlation with CD44 expression. Finally, the *in vivo* behaviour of the developed NP was assessed in a pharmacokinetic study following intravenous administration (IV) in healthy mice.

Materials and methods

Chemicals

Dichloro(1,2-diaminocyclohexane)platinum(II) (DACHPt-Cl₂, $M_w = 380.17$ Da), AgNO₃ ($M_w = 169.97$ Da), mannitol ($M_w = 182$ Da), N1 medium supplement 100X (0.5 mg/mL recombinant human insulin, 0.5 mg/mL, human transferrin - partially iron-saturated-, 0.5 µg/mL sodium selenite, 1.6mg/mL

putrescine, and 0.73 µg/mL progesterone; Sigma-Aldrich)) and Dulbecco's Phosphate Buffer Saline (PBS) were purchased from Sigma-Aldrich (Saint-Quentin-Fallavier, France). Poly-L-Arginine (PA) hydrochloride ($M_w = 5800$ Da) was purchased from Alamanda® Polymers (Huntsville, Alabama, USA). Low molecular weight hyaluronic acid (HA) ($M_w \approx 20$ kDa) was purchased from Lifecore® Biomedical (Chaska, Minnesota, USA). MTS cell titer 96® Aqueous One was provided by Promega (Charbonnières-les-Bains, France). Oxaliplatin solution (Hospira®, Meudon, France) is a kind gift from CHU Angers, France. Alexa Fluor 647 carboxylic acid, TRIS (triethylammonium) salt (0.8 mg/mL) was purchased from Invitrogen (Merelbeke, Belgium). Deionized water (MilliQ water) was obtained from a Milli-Q plus system (Merck-Millipore, Darmstadt, Germany).

DACHPt preparation

DACHPt-Cl₂ was suspended in MilliQ water and mixed with silver nitrate (AgNO₃) to form an aqueous complex ($[AgNO_3]/[DACHPt]=1$) [30]. The solution was kept in the dark under magnetic stirring (500 rpm) at room temperature (22°C) for 24h. Silver chloride precipitates were found after reaction and eliminated by centrifugation at 2,000 g for 20 min at room temperature (22°C). The DACHPt solution was recovered from the supernatant, filtered through a 0.22 µm filter and stored at +4°C.

Preparation of polyarginine hydroxide

Polyarginine hydroxide (PA-OH) solution was prepared from PA-Cl using an Amberlite® IRA 900 Cl ion exchange resin (Sigma Aldrich, Saint Quentin Fallavier, France). Briefly, 3 mL of NaOH (1 M) were added to a column containing 1 mL of wet resin. After 30 min, the column was rinsed with MilliQ water to reach a final pH of 7. Then, PA-Cl solution (50 mg/mL) was added on the top of the column and PA-OH was recovered. The column was rinsed with MilliQ until the solution reached the desired concentration (12.5 mg/mL) and pH around 11. PA-OH stock solution was then stored at +4°C.

Design and development of blank, fluorescent and DACHPt-loaded hyaluronic acid-polyarginine nanoparticles

Blank nanoparticles (NP) made of HA and PA-OH were obtained using the ionic gelation technique [29]. All the solutions were filtered through a 0.22 μm filter prior to their use. To obtain NP, 500 μL of HA solution (concentration ranging from 0.5 to 12 mg/mL, pH = 5) were added to 500 μL of PA-OH solution (concentration 2 mg/mL, pH = 5) and left under magnetic stirring for 5 minutes. To prepare DACHPt-loaded NP, 500 μL of DACHPt (1.5 mg/mL) and 500 μL of PA-OH solution (2 mg/mL) were mixed at stirred at room temperature. Then, 500 μL of HA solution (concentration ranging from 0.5 to 12 mg/mL) were poured over the DACHPt and PA-OH solution, mixed and left under magnetic stirring for 5 min.

Alexa Fluor 647 carboxylic acid was used to label blank HA-PA NP. Prior to obtain NP, 80 μL of PA-OH solution (2.5 mg/mL) and 120 μL of Alexa Fluor 647 carboxylic acid, TRIS (triethylammonium) salt (0.8 mg/mL) were mixed in a glass amber vial with a magnetic stirrer. Then, 100 μL of HA solution (9 mg/mL) was added to the mix and the dispersion was kept under magnetic stirring for 10 minutes. To isolate the NP, 300 μL of the nanocarrier dispersion was transferred to an eppendorf microtube containing 20 μL of glycerol and centrifuged at 16,000 g for 30 minutes at 25°C (Hettich Mikro 220, Sérésin-du-Rhône, France). Subsequently, the supernatant was discarded and the pellet was resuspended in distilled water through vigorous vortexing.

Physicochemical characterization of nanoparticles

Particle size distribution of blank and DACHPt-loaded NP was determined by Dynamic Light Scattering (DLS). Samples were diluted to an appropriate concentration in deionized water and each analysis was carried out at 25°C with an angle detection of 173°. The zeta potential values were calculated from the mean electrophoretic mobility values, as determined by Laser Doppler Anemometry (LDA). For LDA measurements, samples were diluted in NaCl solution (1 mM) and placed in an electrophoretic cell. DLS and LDA analyses were performed on three independently prepared samples using Malvern Zetasizer® apparatus DTS 1060 (Nano Series ZS, Malvern Instruments S.A., Worcestershire, UK). Transmission electron microscopy (TEM) was

performed with a Philips CM120 microscope at “Centre Technologique des Microstructures” (CT μ) at the University of Lyon 1 (Villeurbanne, France). A small drop of suspension (5 μL) was deposited on a carbon/formvar microscope grid (Delta Microscopies, Saint-Ybars, France), stained with a 1% w/w sodium silicotungstate aqueous solution, and slowly dried in open air. The dry samples were observed by TEM under 120 kV acceleration voltage. The osmolality of the formulations was measured using a Wescor Vapro 5520 Vapor Pressure Osmometer (ELITECH group, Signes, France).

Freeze-drying of blank and DACHPt-loaded nanoparticles

Blank and loaded NP were freeze-dried using an ALPHA 1-4 LSC (CHRIST) freeze dryer equipped with RZ6 Vacubrand pump (Fisher Scientific, Illkirch, France). The bulking agent mannitol was prepared at 10 % w/v and used to dissolve HA and dilute PA solutions. The final mannitol concentration in the formulations was around 6% w/v. Size, polydispersity, zeta potential, osmolality, drug loading and entrapment efficiency were evaluated after resuspension of the freeze-dried powders in MilliQ water.

Encapsulation efficiency and loading capacity of DACHPt-loaded nanoparticles

The encapsulation efficiency (EE) was determined indirectly by measuring the unbound DACHPt in the aqueous phase. DACHPt-loaded NP were centrifuged at 7,000 g for 30 min at 20°C (Hettich Mikro 220, Sérésin-du-Rhône, France) using Amicon Ultra-filter (Cut-off 30kDa, Merck Millipore, Cork, Ireland). Supernatants were recovered and analyzed by inductively coupled plasma optical emission spectrometry (ICP-OES). The total amount of drug was estimated from a fresh aliquot of the NP formulation. From the EE values, the loading capacity (LC) of DACHPt-loaded NPs was calculated using the following Equation 1 and 2 respectively:

$$EE (\%) = \frac{\text{Total drug} - \text{Free drug in supernatant}}{\text{Total drug}} \times 100 \quad (1)$$

$$LC (\%) = \frac{\text{Mass of encapsulated drug}}{\text{Mass of the nanoparticles}} \times 100$$

(2)

All measurements were performed in triplicate using DACHPt aqueous solution as control.

Platinum quantification using inductively coupled plasma optical emission spectrometry

ICP-OES measurements were performed on a Thermo Scientific iCAP 7000 Plus Series ICP-OES (ThermoFischer Scientific, Les Ulis, France). Samples were assayed in axial mode, using a plasmaflow of 12 mL/min and nebulizer flow of 0.5 mL/min, in three replicates. Prior to measurement, the samples were diluted in 1% v/v HNO₃. All the standard solutions were daily prepared by diluting the stock solution in 1% v/v HNO₃. Elemental certified stock solutions of 1000 mg/L containing Pt (Merck, Darmstadt, Germany) were used for calibration prior to element analysis by ICP-OES (1–50 mg/L). Emission wave-length λ_{Pt} = 214.4 nm was monitored for Pt, and was based on the best correlation coefficient of the calibration curve. Instrumental limits of detection (LDs) and quantification (LQs) obtained by ICP-OES were calculated following the 3 σ and 10 σ criteria, respectively. Methodological LDs obtained was 0.4 μ g/L by ICP-OES.

Single particle tracking of fluorescent NP (f-NP) in distilled water and human serum

Fluorescence Single particle tracking (fSPT) was used to characterize the diffusion of NP in distilled water and serum. fSPT made use of an iXon ultra EMCCD camera (Andor Technology, Belfast, UK) and swept-field confocal (SFC) microscope (Nikon eclipse Ti, Tokyo, Japan) equipped with an MLC 400 B laser (Agilent technologies, Santa Clara, California, USA) to obtain movies of single fluorescent labelled particles. fSPT measurements on f-NP in biological fluid (90% in volume) were performed as described below. Firstly, the nanoformulations were diluted 15 times in distilled water. Then 5 μ L of the prepared dilution was added to 45 μ L of buffer or human serum (90% vol.) and incubated for 1 h at 37°C. Then, 7 μ L of the sample was mounted on a microscope slide in the middle of a secure-seal adhesive spacer (8

wells, 9 mm diameter, 0.12 mm deep, Invitrogen, Merelbeke, Belgium). The slide was covered by a cover slip (24 \times 50 mm) in order to avoid evaporation of the sample and allow for free diffusion entirely. Subsequently, the slide was placed on the swept field confocal microscope and movies were recorded focused at about 5 μ m above the bottom of the microscope slide. Videos were recorded at room temperature (22.5°C) with the NIS Elements software (Nikon, Tokyo, Japan) driving the EMCCD camera and a swept-field confocal microscope equipped with a CFI Plan Apo VC 100 \times NA1.4 oil immersion objective lens (Nikon, Tokyo, Japan). Analysis of the videos was performed using in-house developed software. Human serum was obtained from a healthy donor as described before [31]. Analyzing movies obtained in fSPT with in-house image processing software [32] as performed in this work led to a distribution of diffusion coefficients, which was converted into size distribution using the Stokes-Einstein equation taking into account the viscosity of the biofluids at which the experiment was performed.

***In vitro* experiments**

Cell lines

B6KPC3 murine pancreatic ductal adenocarcinoma cancer cell line was obtained from the Department of Oncology and Surgical Sciences of Padova University (Italy). B6KPC3 cells were isolated from transgenic mice KPC that spontaneously develop pancreatic ductal adenocarcinoma. B6KPC3 cells medium was composed of Dulbecco's Modified Eagle Medium, DMEM (Lonza, Verviers, Belgium) supplemented with 10% fetal bovine serum (FBS), L-glutamine 2 mM, HEPES buffer 10 mM, 1% of antibiotics (10,000 units penicillin, 10 mg streptomycin, 25 μ g of amphotericin B/mL solubilized in appropriate citrate buffer) and β -mercaptoethanol 20 μ M (Sigma-Aldrich, Saint-Quentin-Fallavier, France). Human lung alveolar carcinoma (A549) were provided by the Cell Bank of the IZSLER (Istituto Zooprofilattico Sperimentale della Lombardia e dell'Emilia-Romagna, Brescia, Italy), these cells were grown in Ham's F12 medium supplemented with 10% FBS, 1 mM glutamine and antibiotics. Human colorectal adenocarcinoma (HT-29) cells were also provided by the Cell Bank of the IZSLER

(Istituto Zooprofilattico Sperimentale della Lombardia e dell'Emilia-Romagna, Brescia, Italy), and were grown in DMEM High (glucose 4.5 g/l) supplemented with 10% FBS, 2 mM glutamine and antibiotics (10,000 units penicillin, 10 mg streptomycin, 25 µg of amphotericin B/mL solubilized in appropriate citrate buffer). Trypsin EDTA (0.05%) was provided by Gibco (Fisher Scientific France, Illkirch, France). All cells were incubated at 37°C at 5% CO₂; after thawing, all the cells were used for less than ten passages.

Viability studies on B6KPC3, A549 and HT-29 cell lines

B6KPC3 cells (3.5×10^3 per well), A549 cells (3.5×10^3 per well) and HT-29 cells (7.5×10^3 per well) were plated into 96-wells plates for 48 h and incubated at 37°C in air controlled atmosphere (5% CO₂) with medium containing serum previously described. The medium was removed and cells were treated for 24 h with increasing concentrations of DACHPt-loaded NP and oxaliplatin solution. Blank NP were also used as control. All the systems were treated with drugs and nanoparticles diluted with serum free N1 supplemented medium. Serum free N1 supplemented medium was prepared with DMEM with amino acids, 1% antibiotics (10,000 units penicillin, 10 mg streptomycin, 25 µg amphotericin B/mL solubilized in an appropriate citrate buffer), 1% HEPES buffer, 1% NEAA (Non Essential Amino Acid) 100X, 1% sodium pyruvate, 1% N1 medium supplement 100X [33,34].

Cell viability reduction assay was performed using CellTiter 96® Aqueous One Solution cell proliferation assay kit containing a tetrazolium compound[3-(4,5-dimethylthiazol-2-yl)-5-(3-carboxymethoxyphenyl)-2-(4-sulfophenyl)-2H-tetrazolium, inner salt; MTS]. Following 24 h of incubation, the medium was removed and cells were incubated with 200 µL of a 1:10 diluted MTS solution. After 2 h at 37°C, the absorbance at 492 nm was recorded using a Microplater Reader (Multiskan Ascent®, Labsystem, Cergy-Pontoise, France for B6KPC3 cells and EnSpire® Multimode Plate Reader, Perkin Elmer, Boston, MA, USA for A549 and HT-29 cells). Cell viability (CV) percentage was evaluated through the following equation 3, with *Absorbance control* well, the absorbance value of untreated cells.

$$CV (\%) = \frac{\text{Absorbance treated well}}{\text{Absorbance control well}} \times 100 \quad (3)$$

CD44 surface receptors assessment on B6KPC3 cell line.

B6KPC3 cells were treated with trypsin EDTA for 2 minutes at 37°C, collected with DMEM 10% FBS and counted. B6KPC3 cells were divided in polypropylene tubes at the density of 5×10^5 cells per tube, centrifuged, washed and resuspended in 100 µL of PBS. Test antibody anti-human/mouse CD44 eFluor® 450 clone IM7 Invitrogen and control antibody EBioscience™ Mo IgG2b k Isotype were provided by eBioscience (ThermoFisher Scientific, Illkirch, France). The antibodies were diluted at a 1:10 ratio, PBS was used as a negative control. Tubes were completed with PBS, incubated 20 min at room temperature. Then, cells were centrifuged, the supernatant discarded and the pellets were reconstituted in PBS and analyzed using a FACS Canto II (BD Biosciences, Le Pont-de-Clay, France).

Evaluation of HMGB1 secretion and ATP release upon incubation of DACHPt-loaded nanoparticles with B6KPC3 cells

B6KPC3 cells were plated and treated as described above, with increasing concentrations of DACHPt-loaded NP, oxaliplatin and DACHPt water solution during 24 h. Blank NP were also tested as a control. The release of damage associated molecular patterns, i.e. HMGB1 and ATP, was assessed [6] in cell culture supernatant using an anti-HMGB1 enzyme-linked immunosorbent assay (ELISA) [35] (IBL International, Hamburg, Germany) and ATP assay [36] (Roche Diagnostics GmbH, Mannheim, Germany), respectively, both were used according to the manufacturer's instructions.

Uptake studies of fluorescent nanoparticles by B6KPC3 cells

B6KPC3 cells were seeded in a 24-well plate at cell density of 5×10^5 cells per well with 500 µL of a complete culture medium. Cells were allowed to grow in an incubator at 37°C in a humidified atmosphere with 5% CO₂. For uptake experiments in biofluid, f-NP (labelled with Alexa-Fluor 647) were dispersed in 90% vol. of human serum and incubated at 37°C for 1 h prior to adding the formulation to the cells.

Subsequently, cells were washed with PBS and incubated in Opti-MEM with f-NP, suspended in biofluid (90% vol.), for 24 and 48h at 37°C. At the end of incubation time, cells were washed twice with PBS, then trypsinized and analysed by Cytoflex (Beckman Coulter, Suarlée, Belgium).

***In vivo* experiments**

Animals

Eight-week-old female C57BL/6 mice were purchased from Charles River Laboratories Inc. (Calco, Italy). All the mice were maintained under specific pathogen-free conditions in the animal facility of the Istituto Oncologico Veneto (Padua, Italy). Animal experiments were performed according to the National and European laws and regulations. All the animal experiments were approved by Padua University Ethical Committee and conducted according to the guidelines of the Federation of European Laboratory Animal Science Association (FELASA). All the animal experiments were in accordance with the Amsterdam Protocol on animal protection and welfare: the mice were monitored daily.

Pharmacokinetic evaluation of DACHPt-loaded NP following intravenous injection

Healthy mice were intravenously (IV) injected with 200 μ L of DACHPt-loaded NP at the dose of 35.9 μ g of platinum equivalent per mouse. Oxaliplatin and DACHPt aqueous solution were used as controls. At specific time points (15 min, 30 min, 1 h, 1.5 h, 3 h, 5 h, 8 h and 12 h), 200 μ L of blood were taken and separated from plasma. Pt content was detected using ICP-OES (ICP-OES ICAP 7200 duo Thermo Scientific). A first compartmental PK analysis was done in Phoenix (Pharsight - a CertaraTM L.P. software 1998-2014, Build 6.4.0.78) using WinNonlin 6.4, Connect 1.4. A first-order two-compartment model with bolus administration, expressed in terms of clearance (CL) and distribution volume (V) was applied to fit the data, using $1/y_{\text{hat}}^2$ as weighting function. The model was either fitted using average data or individual data, and results were comparable in each of the cases.

conditions in order to obtain stable, monodispersed and negatively charged NP (Table 1). Size average distribution of blank-modal distribution <0.2. The ζ potential was negative for all the formulations, around -35 mV.

***In silico* experiments**

Simulation of repeated administration

A multiple administration regimen was simulated using WinNonlin 6.4, Connect 1.4. 8 cycles of 3.5 mg/kg of oxaliplatin solution or DACHPt-loaded NP [37]. The average body weight was 25 g for a mouse and the absolute dose of 87.5 μ g equivalent platinum per mouse. The regimen schedule was: IV infusion (2h) performed on days 1, 4, 8, 11, 15, 18, 22 and 25, a total of two doses per week for 4 weeks.

Statistical analysis

Statistical tests were performed using R (R: A language and environment for statistical computing. R Foundation for Statistical Computing, Vienna, Austria and RStudio (RStudio: Integrated Development for R. RStudio, Inc., Boston, MA, USA). Graphical representation was performed using GraphPad Prism version 6.00 for Windows (GraphPad Software, La Jolla, CA, USA, www.graphpad.com). Normality of the distribution was assessed with Shapiro-Wilk test. When the normality of the distribution was off, non-parametric Kruskal and Wallis tests were performed and the error adjusted with Dunn tests, the type one error rate was taken as alpha = 5% (* p < 0.05).

Results

Development and physicochemical characterization of blank and DACHPt-loaded hyaluronic acid-polyarginine nanoparticles

NP were prepared by polyelectrolyte complexation of negatively charged HA and positively charged PA using the ionic gelation technique [23,38]. In absence of active ingredient, the electrostatic interactions between the carboxylic groups of HA and guanidine groups of PA-Cl led to the formation of the NP. All the formulations were obtained at pH 7.4 to ensure the interaction of the opposite charged polymers. Different polymer ratios were tested to set up the optimal

NP was around 200 nm, and the polydispersity index indicated a mono

Table 1 - Physicochemical properties of blank HA-PA nanoparticles prepared with different mass ratios of [HA]/[PA] (n=3, PDI: Polydispersity Index)

Mass ratio (w/w) HA/PA	Mole ratio HA/PA	Size (nm)	PDI	ζ Potential (mV)										
2.4	8.3	203 ± 8	0.2	-39 ± 9										
2.8	9.7	224 ± 36	0.18	-32 ± 3										
3.2	11.0	220 ± 10	0.16	-35 ± 2										
3.6	12.4	203 ± 3	0.16	-37 ± 2	4	13.8	227 ± 20	0.2	-40 ± 8	4.5	15.5	206 ± 6	0.16	-33 ± 3
4	13.8	227 ± 20	0.2	-40 ± 8										
4.5	15.5	206 ± 6	0.16	-33 ± 3										

To activate DACHPt and to increase its solubility in water, DACHPt-Cl₂ was pretreated with AgNO₃ [(AgNO₃)/(DACHPt) = 1]. The aqueous DACHPt was obtained with a reaction yield of around 70% confirmed by the ICP-OES. Then, DACHPt-loaded NP were formulated by mixing DACHPt solution with the PA-OH solution before adding HA solution (**Figure 1**).

PA-OH was used instead of PA-Cl to produce nanoparticles because chloride ions strongly interfere with the association of DACHPt to

the nanosystem reverting the reaction of drug activation leading to the precipitation of DACHPt-Cl₂. The driving force for DACHPt association to NP was the formation of the metal-polymer complex between platinum and the carboxylic group of the HA in absence of chloride ions, while PA-OH was needed to form stable nanosystems. PA-OH, the cationic polyaminoacid, is a crosslinking agent that allows the formation of stable complexes with high drug encapsulation efficiency as previously reported [38].

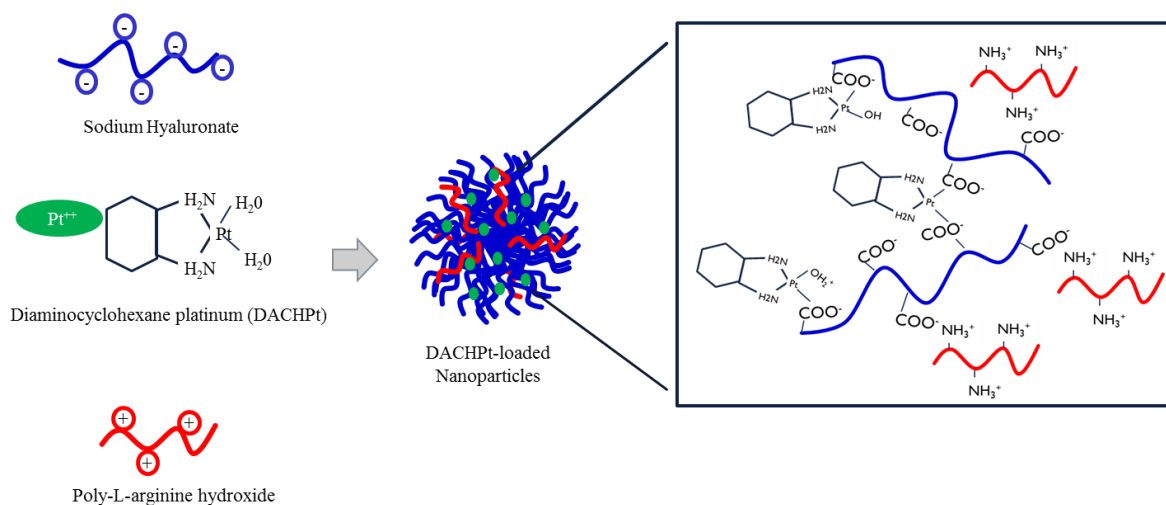


Figure 1 - Schematic representation of DACHPt-loaded NP. .

DACHPt-loaded NP showed a size average distribution between 100 and 170 nm for all the [HA]/[PA] ratios screened (0.2 to 4.8 w/w) (**Table 2**). The presence of the cationic drug DACHPt led to the formation of smaller particles as compared to the blank systems. The polydispersity index (PDI) was in an acceptable range (<0.2) for all the formulations tested indicating that the populations obtained were homogeneous and monodispersed. The ζ potential varied according to the [HA]/[PA] ratio. When the [HA]/[PA] mass ratio was

below 0.2, the surface of the systems was mainly composed of positively charged PA, while, above this ratio, the organization was reversed and HA chains were exposed on the surface leading to a negative surface potential. The stability of DACHPt-loaded NP during storage was assessed following freeze-drying and resuspension in MilliQ water. The cryoprotectant agent selected was mannitol to help the dispersion after reconstitution in water. As shown in **Table 2**, after resuspension, sizes of all the NP increased and

were probably due to the aggregation of nanoparticles during freeze-drying. The encapsulation efficiency of DACHPt to different formulations assessed using ICP-OES, was around 70% for all the systems, and

the drug loading was around 8%. Moreover, the presence of mannitol allowed to obtain an osmolality of around 260 mOsm/kg, a value compatible with an intravenous injection [39].

Table 2 - Physicochemical properties of DACHPt-loaded NP prepared with different mass ratios of [HA]/[PA] before and after freeze-drying (n>5, PDI: Polydispersity Index, EE: entrapment efficiency).

Mass ratio (w/w) HA/PA	Molar ratio HA/PA	Charge ratio HA/PA	Before freeze-drying			After freeze-drying						
			z-Average (nm)	PDI	ζ Potential (mV)	z-Average (nm)	PDI	ζ Potential (mV)	Entrapment Efficiency (EE%)	Drug loading (w/w)	Osmolality (mOsm/kg)	pH
0.2	0.7	1.1	105 ± 3	<0.1	+22 ± 3	NA	NA	NA	NA	NA	NA	NA
1.6	5.5	8.7	130 ± 2	<0.1	-27 ± 2	244 ± 4	<0.1	-42 ± 1	54 ± 3	11 ± 0.7	260 ± 14	5.7
2.8	9.7	15.3	153 ± 2	<0.1	-45 ± 2	235 ± 2	0.12	-46 ± 1	66 ± 4	9 ± 0.6	263 ± 2	5.7
3.6	12.4	19.7	177 ± 3	<0.1	-38 ± 1	242 ± 15	0.10	-44 ± 4	68 ± 0.3	8 ± 0.0	266 ± 9	5.6
4	13.8	21.8	160 ± 1	<0.1	-45 ± 1	241 ± 10	0.11	-41 ± 3	72 ± 2	8 ± 0.2	276 ± 16	5.7
4.5	15.5	24.6	161 ± 4	<0.1	-42 ± 4	238 ± 10	0.11	-46 ± 3	70 ± 3	7 ± 0.3	267 ± 14	5.7
4.8	16.6	26.2	164 ± 3	<0.1	-47 ± 6	236 ± 8	0.10	-40 ± 6	70 ± 1	7 ± 0.1	274 ± 5	5.7

Then, the stability of the systems after reconstitution was studied. The formulation prepared at the HA/PA ratio of 4.5 remained stable without significant change in terms of size and PDI for 4 weeks after reconstitution

(**Figure 2**). This result indicated that the selected formulation could have a strong potential as drug delivery system and was retained for further studies.

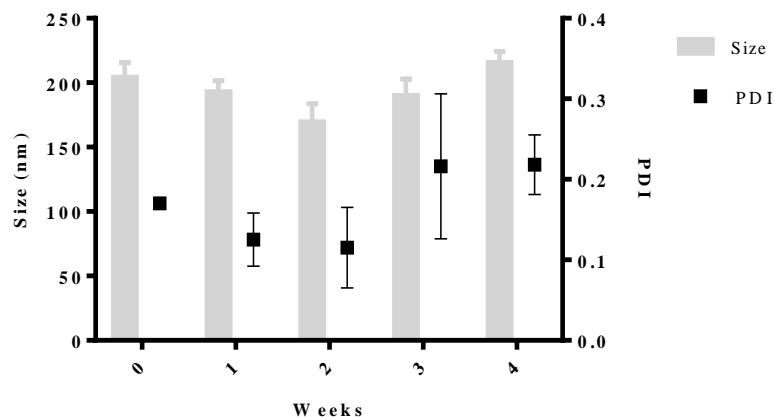


Figure 2 – Size and PDI of freeze-dried DACHPt-loaded nanoparticles (polymer mass ratio [HA]/[PA] = 4.5) after reconstitution (mean \pm SD, n=3).

To analyze the morphological structure of blank and DACHPt-loaded NP, transmission electron microscopy (TEM) analyses were performed. The images obtained after freeze-drying of the NP and resuspension in water are showed in **Figure 3**. Both blank and DACHPt-loaded NP formed well-defined and

homogeneous structures with spherical shape. The sizes measured confirmed those obtained by DLS analysis (around 250 nm). Following reconstitution in water, some aggregates appeared, confirming the increase in size observed by DLS after freeze-drying.

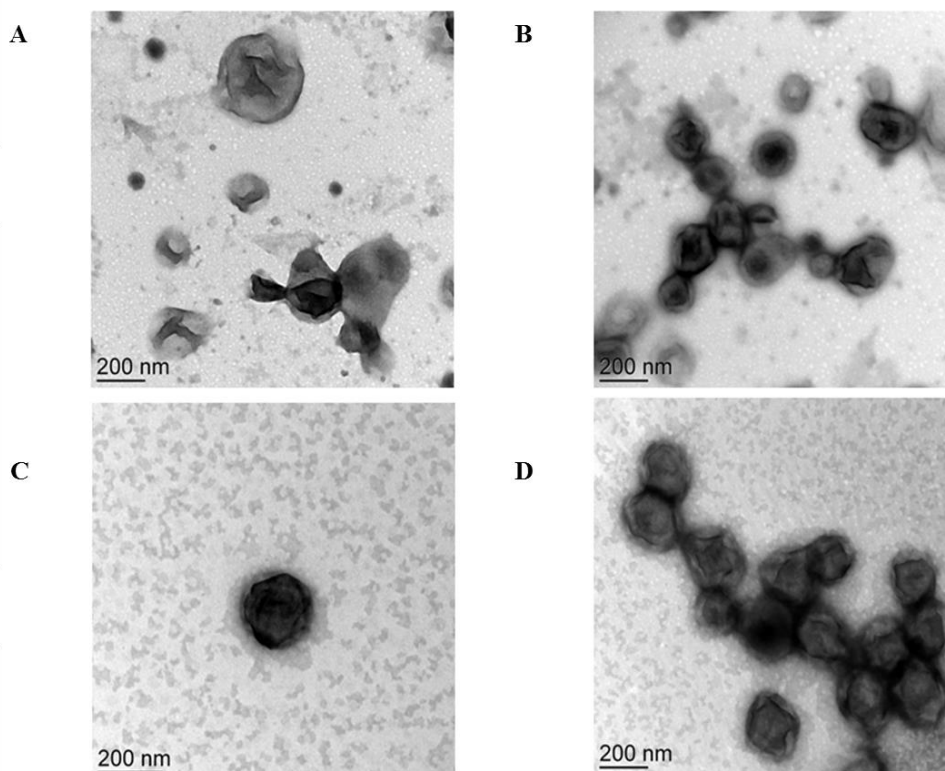


Figure 3 - TEM of DACHPt-loaded nanoparticles after freeze-drying (A and B) and blank nanoparticles (C and D). (Scale bar is 200 nm and operating voltage = 120 kV).

Once the system was optimized, single particle tracking analysis was performed to assess the stability of the NP upon incubation in human serum. **Figure 4** shows that when fluorescent NP (f-NP) were diluted in MilliQ water, an average size of 266 nm was detected. This result was consistent with the DLS values and was also close to the values obtained by TEM

observations. Also, after incubation in 90% volume of human serum for 1 hour at 37°C, NP showed a narrow size distribution with an average size of 275 nm. The results demonstrated the colloidal stability of NP under biological conditions which is pivotal for biomedical applications.

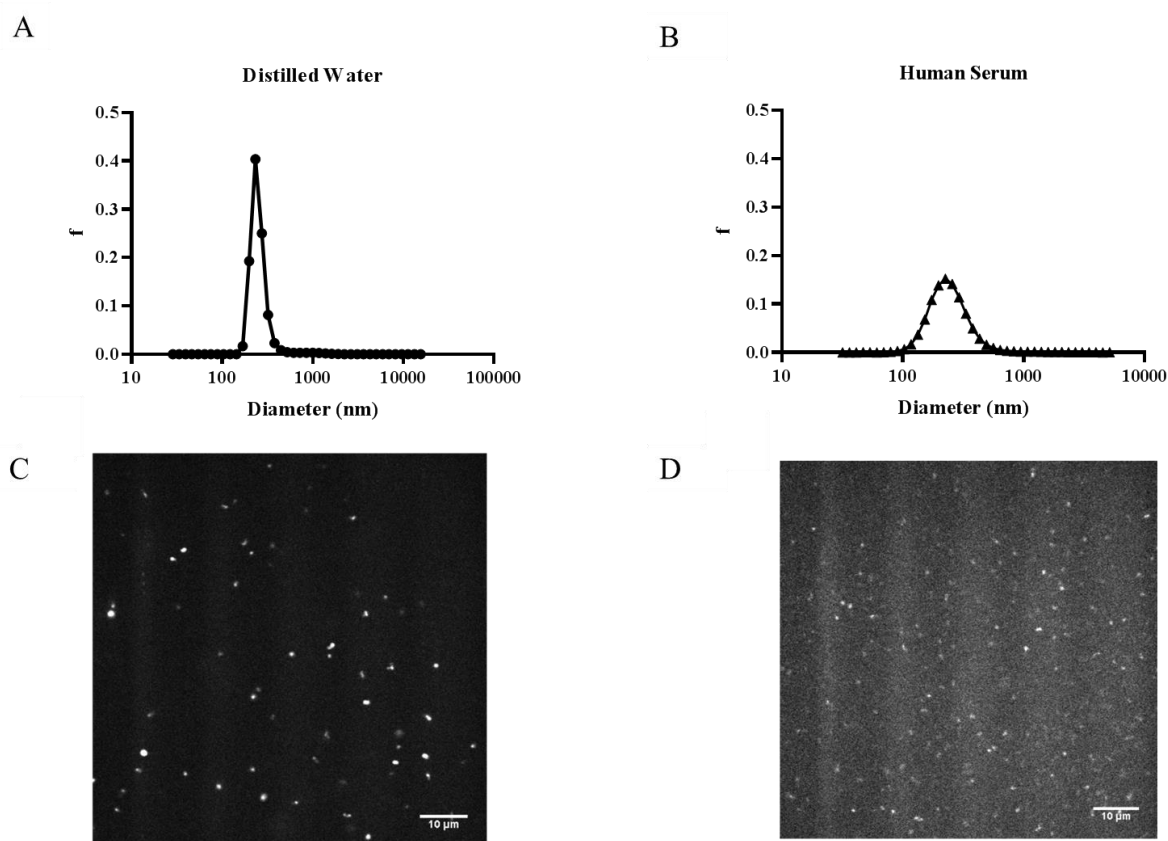


Figure 4 – Single particle tracking size measurements of fluorescent NP (f-NP) after 1 hour incubation in distilled water (A) and human serum (B). Snapshots of the movies showing f-NP dispersed in distilled water (C) and in human serum (D).

***In vitro* cytotoxic evaluation of DACHPt-NP**

To assess the efficacy in viability reduction of DACHPt-loaded NP on different tumor cell lines, MTS test was used. B6KPC3, HT29 and A549 cells were treated with DACHPt-loaded NP, and oxaliplatin at drug concentrations ranging from 1 μM to 200 μM during 24 h (**Figure 5**). Blank NP, at the same concentrations as DACHPt-loaded NP were tested to assess the biocompatibility of the nanocarrier. *In vitro* cytotoxicity studies (**Table 4**) revealed that DACHPt-loaded NP were able to reduce cell viability for all the

cancer cell lines tested. In the case of B6KPC3 cells, IC₅₀ of DACHPt-loaded NP was 1.3 times lower (18 vs 23 μM) in comparison to the oxaliplatin solution. In the case of HT-29, the IC₅₀ was reduced by a factor of 2 as compared to the reference oxaliplatin solution (IC₅₀ of 39 vs 74 μM, respectively), while NP toxicity was comparable with the oxaliplatin reference solution in A549 cell lines (IC₅₀ 11 and 12 μM, respectively). Blank NP did not interfere with cell viability at all the concentrations tested.

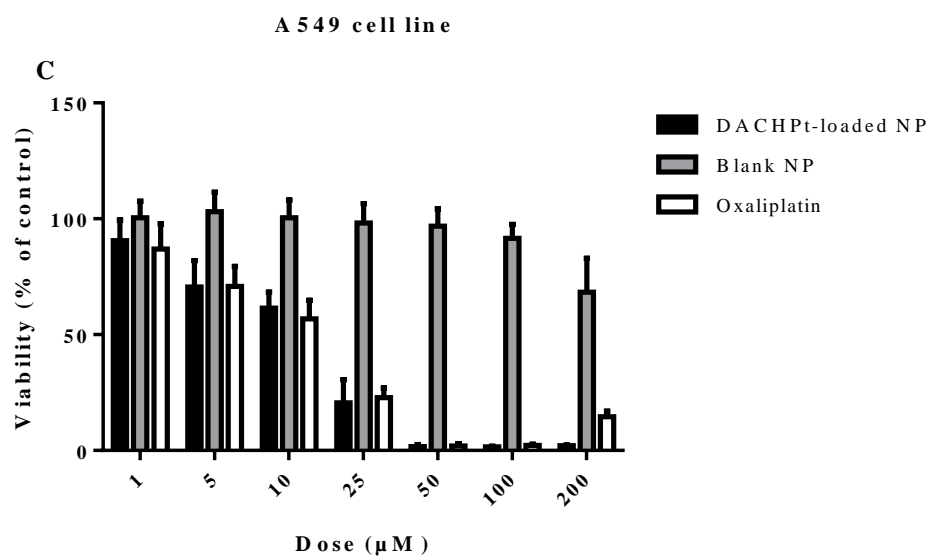
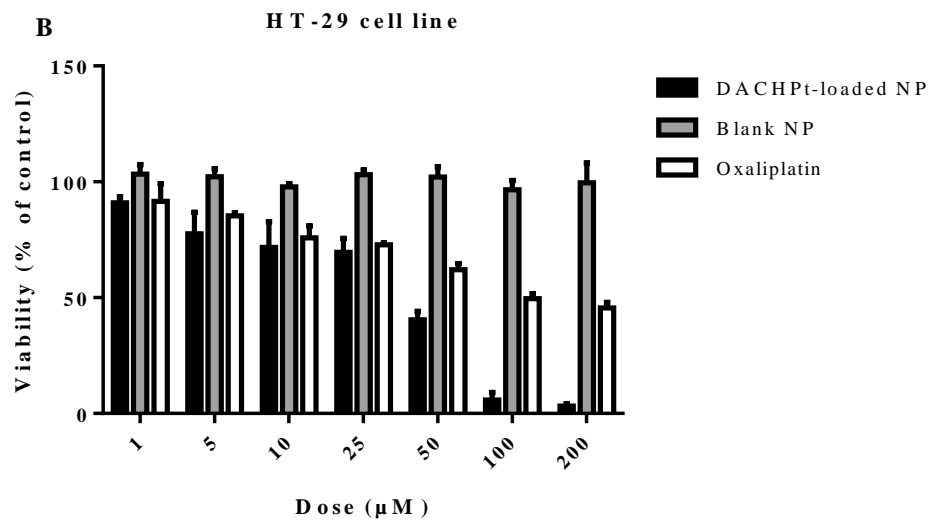
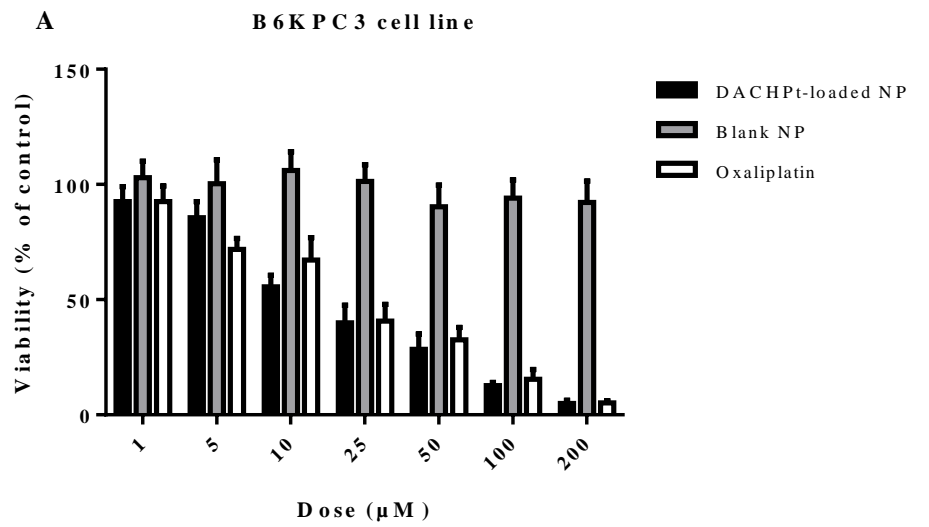


Figure 5 - Viability assessment performed on B6KPC3 (A), HT-29 (B) and A549 (C) cells after 24 h of incubation at 37°C with increasing concentrations (0 - 200 μ M) of oxaliplatin, blank NP and DACHPt-loaded NP for 24 h (Mean \pm SD, n=6 (A) & n=3 (B and C)) (a boxplot representation of B6KPC3 cells plot can be found in *supplementary data*).

Table 4 – Calculated IC50 for B6KPC3, HT-29 and A549 cells lines after 24h of incubation at 37°C with increasing concentrations (0 - 200 μ M) of DACHPt-loaded nanoparticles, oxaliplatin and DACHPt solutions. (Mean \pm SD, n=6 (B6KPC3) & n=3 (HT-29 and A549))

Cell line	Oxaliplatin	DACHPt-loaded NP
B6KPC3	23 μ M \pm 1.0	18 μ M \pm 1.1
HT-29	74 μ M \pm 2.9	39 μ M \pm 2.3
A549	11 μ M \pm 2.2	12 μ M \pm 1.2

Assessment of CD44 expression at B6KPC3 cell surface and cellular uptake of fluorescent nanoparticles in biofluids

Cell internalization of HA decorated systems can occur through CD44 binding as demonstrated for colon and lung cancer cell lines [40,41]. To assess if CD44 was also expressed on B6KPC3 cells and hence could

trigger NP internalization, cytometry analysis was performed. An isotype control was used to assess non-specific binding. The CD44 appeared to be expressed at the surface of the B6KPC3 cells (**Figure 6A**). This result indicated that HA decorated nanosystems could be efficient to target these cells.

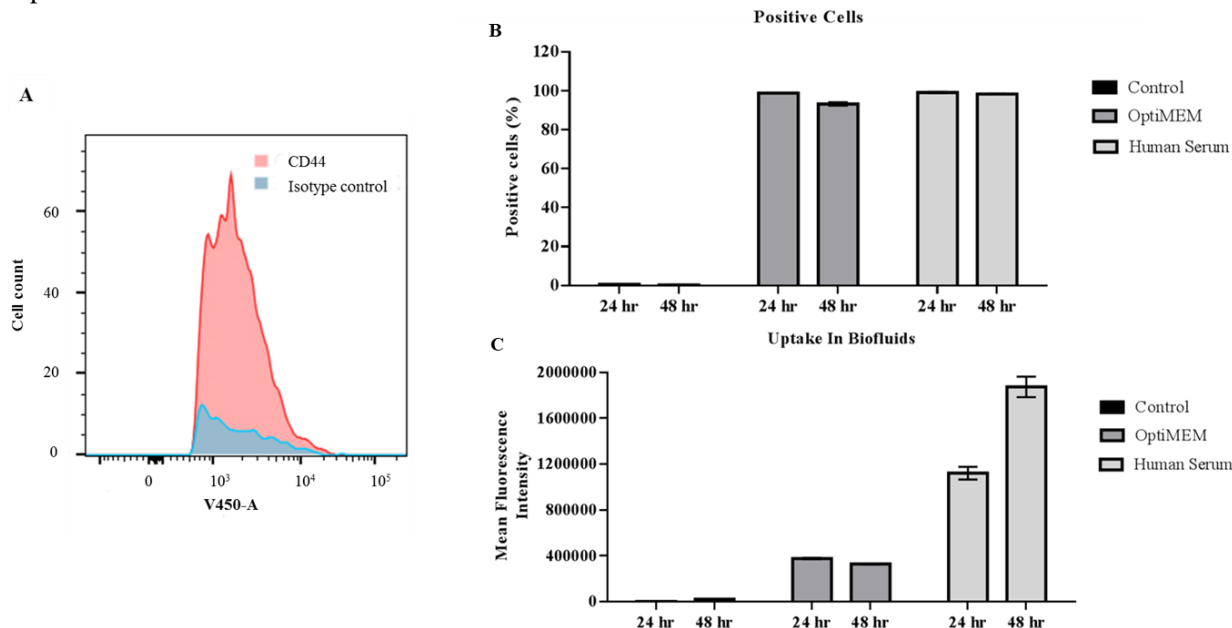


Figure 6 – (A) Histogram for CD44 expression at the surface of B6KPC3 cells (red), 1.10^5 cells were gated per condition. An isotype control (blue) was used to assess the non-specific binding. The binding is expressed as a cell count according to the fluorescence intensity obtained with the selected laser (V450-A). (B and C) Uptake studies of f-NP by B6KPC3 cells in culture media (control), OptiMEM and human serum. (Mean \pm SD, n=3)

The uptake of f-NP was studied using B6KPC3 cells in presence of biofluids such as serum-free medium (OptiMEM) and human serum. **Figure 6B and 6C** revealed that f-NP were highly uptaken by B6KPC3 cells in presence of 90% volume of biofluids. All the cells

displayed a positive fluorescence signal indicating that 100% of the cells internalized the labelled NP in the OptiMEM and human serum at 24 h. The cellular uptake increased in human serum compared to OptiMEM. After 48 h, the cellular uptake declined in OptiMEM

while mean fluorescence intensity remained stable following incubation in human serum suggesting that the f-NP were more uptaken by B6KPC3 in media with human serum.

Improved ability of DACHPt-loaded NP to induce HMGB1 secretion *in vitro*

Recently, it has been reported that oxaliplatin can induce the immunogenic cell death (ICD) of tumor cells [6,42]. It was suggested that nanoparticles loaded with DACHPt may impact ICD due to their proven advantages in delivery the chemotherapeutic drug to cancer cells. Major signs of ICD are the extracellular release of adenosine triphosphate (ATP), and

the passive release of chromatin-binding protein high mobility group B1 (HMGB1). Therefore, the ability of DACHPt-loaded NP, oxaliplatin and DACHPt to induce HMGB1 release after 24 h of incubation with B6KPC3 cells was evaluated (Figure 7). At low drug concentration (1 μM), no HMGB1 release was observed for all the treatments. Besides, at high concentration (50 and 500 μM of DACHPt) loaded NP significantly increased HMGB1 release from B6KPC3 cells. In the case of ATP release, no differences were found among the different conditions tested (data not shown).

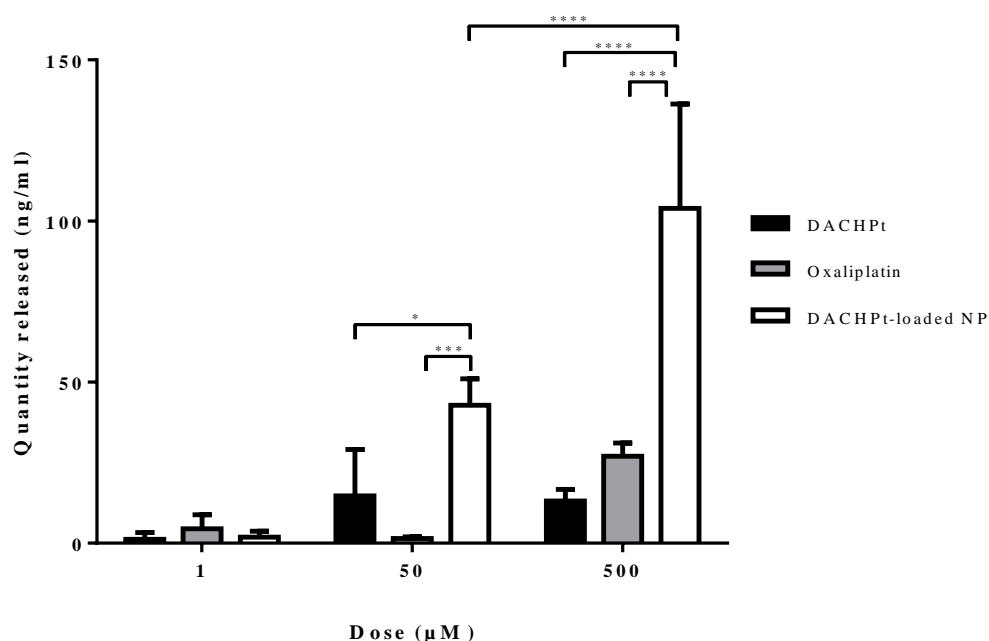


Figure 7 – HMGB1 release by B6KPC3 cells after 24 h of treatment with DACHPt-loaded NP, oxaliplatin or DACHPt water solution. (Mean \pm SD, n=3)

In vivo experiments: pharmacokinetic studies in healthy mice

In order to study the pharmacokinetic behavior of DACHPt-loaded NP, healthy mice were intravenously injected (IV) with DACHPt-loaded NP. Oxaliplatin solution at the same dose was used as a control. Platinum (Pt) and DACHPt concentrations were quantified using ICP-OES as described above. Pt concentration derived from oxaliplatin solution and DACHPt concentration derived from DACHPt-loaded

NP were plotted as a function of time (Figure 8) and data were analyzed using a two-compartmental model. As shown by the plasma level-time curves, free oxaliplatin or encapsulated DACHPt showed a biphasic pattern, which resulted from the extensive distribution of platinum derivatives into different tissues, followed by their terminal elimination from the body.

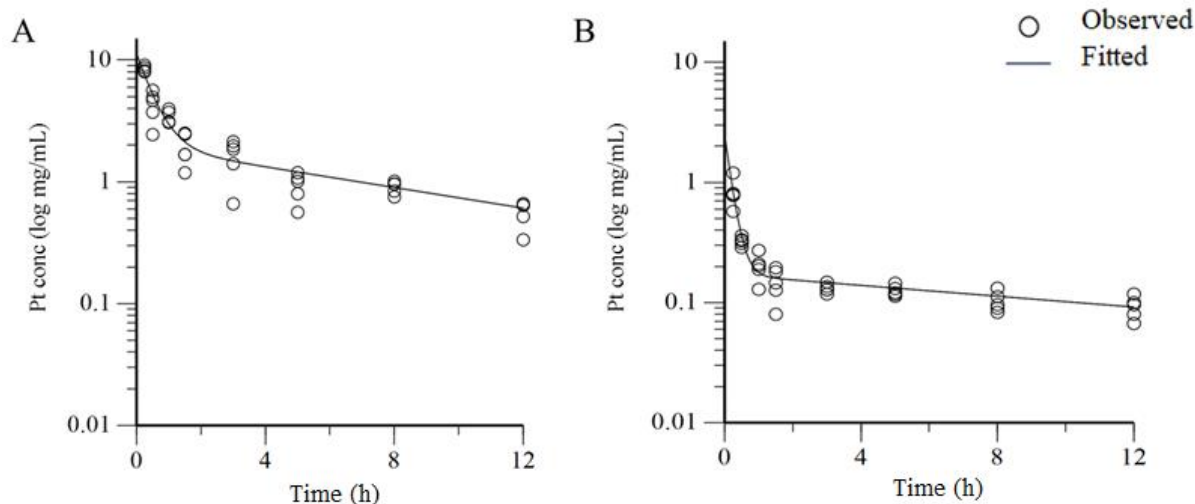


Figure 8 - Plasma concentration-time curves of Pt derivatives after IV bolus injection of 35.9 μg DACHPt-loaded NP (A) or oxaliplatin solution (B) to mice. The circles show the observed plasma concentrations in the individuals, while the line represents the best fit through the data. Parameters obtained from the fitted curves are displayed in **Table 5**.

As reported in **Table 5**, the Area Under the Curve (AUC) following the administration of DACHPt-NP was 24 $\text{h} \cdot \text{mg/L}$, six times higher than the value obtained following the administration of oxaliplatin solution, which was 3.76 $\text{h} \cdot \text{mg/L}$. The C_{max} , defined as the maximal drug concentration detected in the blood at time 0h was 11.4 mg/L for NP and 2.48 mg/L for oxaliplatin solution, almost five times higher than the control drug.

The distribution half-life (alpha half-life) indicated that when the drug was entrapped into NP, it was distributed slower than oxaliplatin (0.370 h for NP vs 0.135 h for oxaliplatin solution). However, the elimination rate (beta half-life) was more rapid for NP in comparison to oxaliplatin solution (6.49 h for NP vs 13.6 h for oxaliplatin solution). The results showed that the Pt concentration in plasma started at a lower level and initially

decreased much more rapidly for the oxaliplatin solution as compared to the NP.

K_{12} (rate constant of distribution from central to peripheral compartment) was higher for oxaliplatin solution as compared to the one obtained with DACHPt NP (4.14 vs 1.08 h^{-1}). K_{21} (rate constant of distribution from peripheral compartment to central compartment) was similar for oxaliplatin and DACHPt NP (0.398 and 0.418 h^{-1}). Volume of distribution of the central and peripheral compartment (V_c 0.003 and V_p 0.008 L for the NP vs V_c 0.014 and V_p 0.150 L for oxaliplatin solution) as well as the volume of distribution at steady state (V_{ss}) of the NP were lower with respect to the oxaliplatin solution (0.011 vs 0.165 L). Plasma clearance differed by a factor of five, being 0.002 and 0.010 L/h for NP and oxaliplatin solution, respectively.

Table 5 - Pharmacokinetic parameters obtained following IV bolus injection of an equivalent dose of a 35 μg Pt/mouse of DACHPt-loaded NP or oxaliplatin solution.

Parameters	Units	DACHPt-loaded NP	Oxaliplatin
		Calculated values	
AUC	$\text{h} \cdot \text{mg/L}$	23.8 ± 1.52	3.76 ± 0.52
Alpha half-life	h	0.370 ± 0.075	0.135 ± 0.023
Beta half-life	h	6.49 ± 1.08	13.60 ± 2.89
K_{12}	1/h	1.08 ± 0.26	4.14 ± 0.72
K_{21}	1/h	0.418 ± 0.088	0.398 ± 0.054

C _{max}	mg/L	11.4 ± 1.82	2.48 ± 0.68
AUMC	h*h*mg/L	178 ± 37.8	65.1 ± 23.8
V _{ss}	L	0.011 ± 0.001	0.165 ± 0.018
V _c	L	0.003 ± 0.0005	0.014 ± 0.004
CL	L/h	0.002 ± 0.0001	0.010 ± 0.001
V _p	L	0.008 ± 0.001	0.15 ± 0.02

Then, in order to study the maintenance of drug therapy, a repeated administration regimen was simulated. The repeated administration schedule was intended to minimize side effects while maintaining therapeutic drug concentration in plasma. In order to simulate an *in vivo* multiple administration regimen, a protocol constituting

of 8 cycles of 3.5 mg/kg of oxaliplatin solution or DACHPt-loaded NP was established [43]. In **Figure 9**, concentrations of Pt from oxaliplatin solution or from DACHPt-loaded NP as well as DACHPt, were represented as a function of time as linear scale (y-axis), or semilog scale (y-axis).

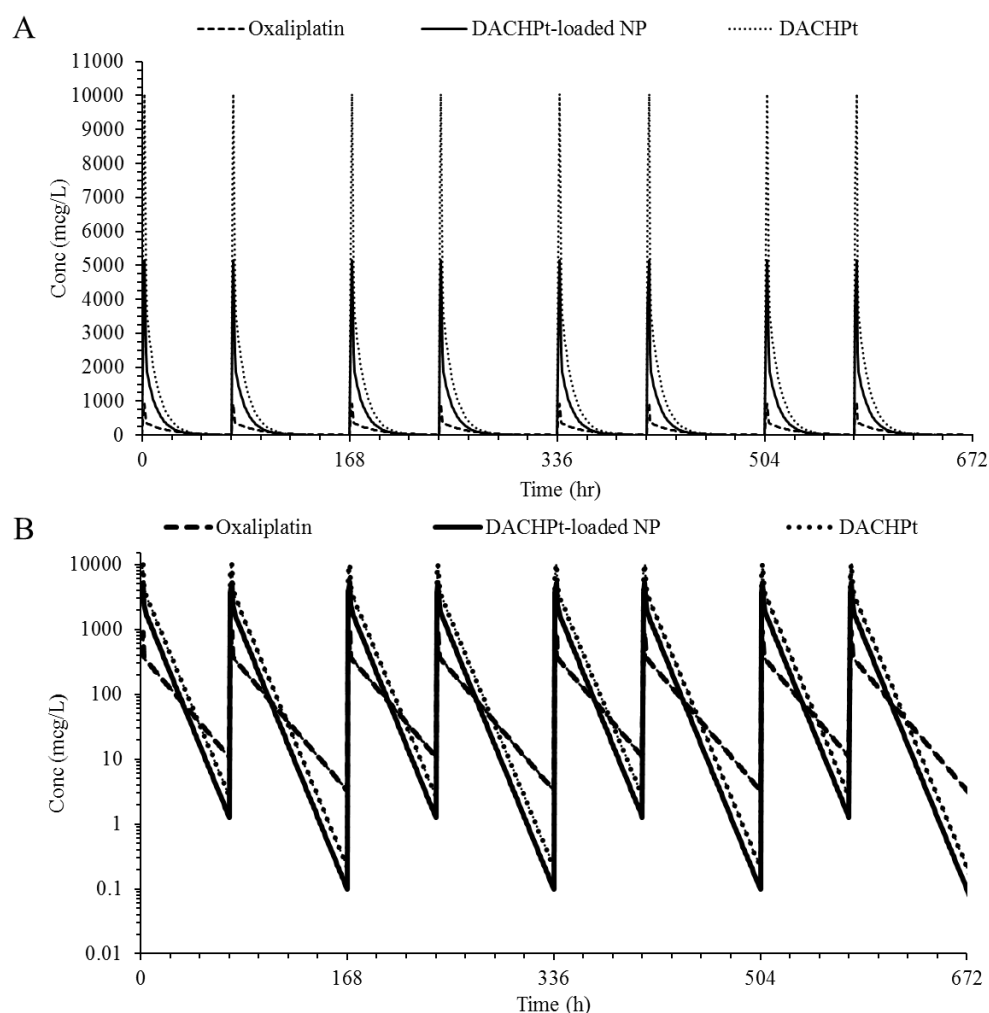


Figure 9. Plasma concentration-time curves of platinum derivatives after 2 h of IV infusion of multiple administrations (twice a week for 4 weeks) of 3.5 mg/kg of oxaliplatin solution or DACHPt-loaded NP (“-” for DACHPt detection and “...” Pt detection) or oxaliplatin solution to mice. (B) Plasma concentration-time curves (concentration is plotted on a log scale) of Pt derivatives after 2 h of

repeated IV infusion of 3.5 mg/kg of oxaliplatin solution or DACHPt-loaded NP (“-” for DACHPt detection and “...” Pt detection) or oxaliplatin solution in mice.

From **Figure 9**, it can be noticed that there was no accumulation of Pt with the selected regimen and the drug was always eliminated before the next administration. Plasma drug concentration fluctuations were observed for all the treatments tested. Finally, steady state was rapidly reached for all the compounds with two injections per week for four weeks regimen.

Discussion

Chemotherapy regimens using platinum drugs are highly effective and widely used for the treatment of several malignancies. However, the improvement of specific delivery to tumors is required to increase therapeutic drug levels in pathological sites and to reduce side effects associated with unspecific drug distribution [44]. In this field, polymer nanosystems made of bioinspired materials represent an attractive strategy due to their biocompatibility, tunable design, possibility to load a wide range of molecules and ability to selectively accumulate in solid tumors [45]. The aim of this work has been to develop and characterize nanoparticles made of HA and PA as a versatile platform for the encapsulation of hydrophilic actives, as platinum derivatives. To reach this objective, an exhaustive physico-chemical characterization of the nanosystem has been developed aimed at selecting the suitable parameters to obtain stable NP. Moreover, to increase their shelf-life and to facilitate their handling and storage, a freeze-drying process was investigated.

NP were obtained using the ionic gelation technique which is based on the electrostatic interactions between the positively charged primary amino groups of PA and the negatively charged carboxylic groups of HA. The optimal blank formulation in terms of stability had a HA/PA mass ratio of 4.5, yielded particles with an average size of 206 nm, a PDI ≤ 0.2 and a negative zeta potential (-35 mV). In the case DACHPt-loaded NP, the modification of polyarginine chloride was required to obtain chlorine free PA and hence facilitate the encapsulation of the drug in the nanosystems. Finally, particles with an average size of 161 nm, a PDI ≤ 0.2 and a negative zeta potential (-42 mV) were obtained. The

reduction in size of drug-loaded nanoparticles, already observed with other actives, is related to the attractive forces that modulates electrostatic interactions within the complexes in presence of activated DACHPt [38]. This process allowed the formation of nanoparticles in a fast and simple process paving the way for a future scale up of the technology, with no need for chemical synthesis.

To stabilize the system during freeze-drying and to obtain a fluffy white cake easily resuspendable in water, mannitol was used as a cryoprotectant and bulking agent. Following resuspension, the physicochemical characteristics of NP in terms of size, PDI and drug loading were maintained. NP showed an average size of 238 nm and a PDI ≤ 0.12 , this slight increase in size measured in DLS might be due to some NP aggregation as observed in TEM image, while, the entrapment efficiency was above 70%. To assess the integrity of NP in complex media such as human plasma, SPT has been used to monitor the size of nanosystems in undiluted biofluids [32,46,47]. fSPT gave comparable size distributions to DLS for NP assayed in colloidal suspension (around 200 nm). Upon 48h of incubation NP maintained their size in human plasma suggesting *in vivo* stability of the carriers.

Then *in vitro* experiments were carried out to evaluate the anticancer activity of DACHPt-loaded NP in colon (HT-29), lung (A549) and pancreatic (B6KPC3) cancer cell lines following 24h of incubation. In HT-29 cells, the IC₅₀ of DACHPt-loaded NP was 2 times lower in comparison to the value obtained with oxaliplatin (39 μ M and 74 μ M). In B6KPC3 cells, the IC₅₀ value was also lower than oxaliplatin solution (18 μ M and 23 μ M), whereas DACHPt-loaded NP and oxaliplatin had comparable toxicity in A549 cell line (12 μ M and 11 μ M). At all the concentrations tested, blank NP did not affect cell viability highlighting their biocompatibility. These results suggest that HA-PA NP is an effective carrier in enhancing anticancer activity of associated DACHPt. Besides, for a short incubation time (24 h), nanocarriers encapsulating drug showed higher *in vitro* cytotoxicity when compared to the free drug. Also, Tsai *et al.* showed that poly(amidoamine)-polyglutamic acid-b-D-a-

tocopheryl polyethylene glycol 1000 succinate worked more effectively than oxaliplatin did on A549 cells at 24 h [48]. While, Murakami, *et al.* observed that DACHPt-loaded micelles made of polyglutamic acid and PEG displayed a value of IC₅₀ against HT29 cells lower than that of oxaliplatin by a factor of 4.7 following 48 h of treatment [15]. In the case of micelles made of dendritic block copolymer poly-(amidoamine)-polyglutamic acid-b-polyethylene glycol (PAM-PG₁ub-PEG) and loaded with DACHPt the enhancement of cytotoxicity was reached only after 72 h of incubation [49]. This reduction in cell viability could be ascribed to an enhanced internalization of NP via CD44/HA interaction. HA is known to be a ligand of different CD44 isoforms overexpressed by a large panel of cancer cell lines including pancreatic, lung and colon cancer cell lines [50,51]. The involvement of CD44 in the progression of lung and colon cancer, has been largely described, while there were only a few reports regarding the interaction of CD44 in pancreatic cancer cell lines [52]. The interactions between the polymer free in solution, grafted to liposomes or coated in NP, can create stronger binding to CD44 receptors. Longer HA chains have multiple interactions with CD44 molecules, leading to an increase in affinity, and in enhancement of HA internalization into cells. However, long HA chains are rapidly cleared from the circulation by the hyaluronan receptor for endocytosis (HARE) which is present on liver sinusoidal endothelial cell [52]. In this study, a low molecular weight HA (20 kDa) was selected, the HA was long enough to bind to CD44 but too short to bind to the HARE receptor. By means of FACS analysis, it was disclosed that B6KPC3 expressed CD44 receptor and the internalization by these cells could be driven by receptor recognition. Internalization experiments in B6KPC3 cells confirm that cells treated with f-NP highly expressed fluorescence; therefore, they internalized f-NP in a high amount.

In addition to a direct cytotoxic effect, DACHPt-loaded NP induced signals related with ICD. ICD is a form of cell death that triggers a T cell-dependent immune response depending on a temporal sequence emission of damage-associated molecular patterns (DAMPs) such as ATP, calreticulin (CTR) and high mobility group box 1 (HMGB1) [53,54].

The emission of those DAMPs enhances the immunogenicity of dying cells leading to an anticancer immunity responses [55]. It has been reported the efficacy of oxaliplatin based treatments inducing increased HMGB1 release and ATP secretion in pancreatic cells Panc-1 and Pan02 cells after 48 h of exposure [7]. Here it was demonstrated that DACHPt-loaded nanoparticles can induce ICD also on B6KPC3 enhancing HMGB1 release and ATP release after 24 h of incubation. Altogether, these results indicated that NP encapsulation is a powerful method to increase DAMPs exposure improving drug cytotoxicity *in vitro*.

Finally, DACHPt-loaded NP and oxaliplatin solution were injected intravenously and the plasma concentrations quantified to determine the pharmacokinetic behavior of the formulations. The PK of platinum in plasma ultrafiltrate after oxaliplatin administration is characterized by a short initial distribution phase and a long terminal elimination phase. In clinical studies, it was observed that at the end of a 2 h oxaliplatin infusion, only 15% of the administered Pt was present in the systemic circulation [56]. As reported in the literature, once injected, Pt binds irreversibly to plasma proteins (predominantly serum albumin) and erythrocytes. The erythrocytes did not serve as a reservoir for Pt in the systemic circulation, and accumulation of Pt in blood cells is not considered to be of clinical relevance [56].

On the contrary, following the administration of DACHPt-loaded NP, AUC and C_{max} values are 6 and 5 times higher respectively, than the values obtained following the administration of oxaliplatin solution. The alpha and beta half-lives indicated that DACHPt-loaded NP were distributed more slowly (0.37 h vs 0.135 h for oxaliplatin) but eliminated more rapidly than the reference oxaliplatin solution (6.49 h vs 13.60 h for NP and oxaliplatin solution, respectively).

So far, a significant effort have been spent on developing long circulating nanoparticle formulation able to enhance the plasmatic half-life of the associated drugs [12]. Prolonged circulation could also mean slow tissue distribution of the nanoparticles (including to the target tissue) and very slow drug release. A right balance between long circulating properties, distribution and elimination rates is hence needed to avoid side effects and indiscriminate accumulation [57]. In the case of nanoparticles, the achievement of higher

exposures during and immediately post dosing is evident. Then, the drug concentration decreased rapidly for both oxaliplatin solution and DACHPt-loaded NP.

From a simulated multiple administration regimen of DACHPt-loaded NP, there was no accumulation of Pt and steady state was rapidly reached for all the moieties plotted. Generally, in a repeated administration schedule, accumulation can occur when the drug is administered before the previous dose is completely eliminated. Then, the amount of drug in the body will progressively rise. From **Figure 9** it can be observed that the drug was always eliminated without relevant accumulation. However, in the case of DACHPt-loaded NP, a higher exposure was maintained for at least two days, while in the case of oxaliplatin solution the amount of the drug detected in the blood was quite low even at the starting point.

Globally, the results presented here are associated with a high stability, slower *in vivo* release and clearance of the nanoparticles as compared to the drug alone.

Conclusion

This present work disclosed a novel nanosystem made of HA-PA NP for the encapsulation of DACHPt. This system was stable in human serum, could be lyophilized, and after reconstitution in water the physicochemical properties as size, polydispersity, and osmolality were still compatible with IV injection. The anticancer activity *in vitro* both in terms of cytotoxic activity and ICD inducer, of DACHPt was enhanced by its encapsulation in the HA-PA nanoparticles, while blank nanosystems did not show any toxicity. Moreover, due to the HA coating, it could be suggested that nanoparticles might be internalized via CD44 in B6KPC3 cell. *In vivo* pharmacokinetic studies showed that following IV injection of DACHPt-loaded NP a slower drug release, associated to a lower elimination and distribution of the drug as compared to oxaliplatin solution, occurred. These observations suggest that tunable nanomedicines based on bioinspired polymers have the potential to enhance drug efficacy and be more effective than oxaliplatin alone.

Acknowledgements

This work has been carried out within the research program NICHE, financially supported by EuroNanoMed-II (4th call).

Declaration of interest

The authors declare no conflict of interest

Bibliography

- [1] H.S. Oberoi, N. V. Nukolova, A. V. Kabanov, T.K. Bronich, Nanocarriers for delivery of platinum anticancer drugs, *Adv. Drug Deliv. Rev.* 65 (2013) 1667–1685. doi:10.1016/j.addr.2013.09.014.
- [2] L. Kelland, The resurgence of platinum-based cancer chemotherapy, *Nat. Rev. Cancer.* 7 (2007) 573. <https://doi.org/10.1038/nrc2167>.
- [3] E. Wiltshaw, Cisplatin in the Treatment of Cancer, *Platinum. Met. Rev.* 23 (1979) 90–98.
- [4] E. Raymond, S.G. Chaney, A. Taamma, E. Cvitkovic, Oxaliplatin: A review of preclinical and clinical studies, *Ann. Onc.* 9 (1998) 1053–1071. doi:10.1023/A:1008213732429.
- [5] P.M. Bruno, Y. Liu, G.Y. Park, J. Murai, C.E. Koch, T.J. Eisen, et al., A subset of platinum-containing chemotherapeutic agents kill cells by inducing ribosome biogenesis stress rather than by engaging a DNA damage response Peter, *Nat Med.* 23 (2017) 461–471. doi:10.1038/nm.4291.
- [6] A. Tesniere, F. Schlemmer, V. Boige, O. Kepp, I. Martins, F. Ghiringhelli, et al., Immunogenic death of colon cancer cells treated with oxaliplatin, *Oncogene.* 29 (2010) 482–491. doi:10.1038/onc.2009.356.
- [7] X. Zhao, K. Yang, R. Zhao, T. Ji, X. Wang, X. Yang, et al., Inducing enhanced immunogenic cell death with nanocarrier-based drug delivery systems for pancreatic cancer therapy, *Biomaterials.* 102 (2016) 187–197. doi:10.1016/j.biomaterials.2016.06.032.
- [8] S.R. McWhinney, R.M. Goldberg, H.L. McLeod, Platinum neurotoxicity pharmacogenetics, *Mol. Cancer Ther.* 8 (2009) 10–16. doi:10.1158/1535-7163.MCT-08-0840.
- [9] N.T. Phan, A.E. Heng, A. Lautrette, J.L. Kémény, B. Souweine, Oxaliplatin-induced acute renal failure presenting clinically as thrombotic microangiopathy: think of acute tubular necrosis, *NDT Plus.* 2 (2009) 254–256. doi:10.1093/ndtplus/sfp008.
- [10] C. Duvic, D. Sarret, F. Didelot, G. Nédélec, J. Labaye, L.-H. Noël, et al., Renal toxicity of Oxaliplatin, *Nephrol. Dial. Transplant.* 20 (2005) 1275–1276. doi:10.1093/ndt/gfh826.
- [11] Y. Mochida, H. Cabral, K. Kataoka, Polymeric Micelles for Targeted Tumor Therapy of Platinum Anticancer Drugs, *Expert Opin. Drug Deliv.* 00 (2017) 17425247.2017.1307338. doi:10.1080/17425247.2017.1307338.
- [12] H. Cabral, N. Nishiyama, S. Okazaki, H. Koyama, K. Kataoka, Preparation and biological properties of dichloro(1,2-diaminocyclohexane)platinum(II) (DACHPt)-loaded polymeric micelles., *J. Control. Release.* 101 (2005) 223–232.

- doi:10.1016/j.jconrel.2004.08.022.
- [13] H.S. Oberoi, N. V. Nukolova, Y. Zhao, S.M. Cohen, A. V. Kabanov, T.K. Bronich, Preparation and *In Vivo* Evaluation of Dichloro(1,2-Diaminocyclohexane)platinum(II)-Loaded Core Cross-Linked Polymer Micelles, *Chemother. Res. Pract.* 2012 (2012) 1–10. doi:10.1155/2012/905796.
- [14] Z. Hang, M.A. Cooper, Z.M. Ziora, Platinum-based anticancer drugs encapsulated liposome and polymeric micelle formulation in clinical trials, *Biochem. Compd.* 4 (2016) 1. doi:10.7243/2052-9341-4-2.
- [15] M. Murakami, H. Cabral, Y. Matsumoto, S. Wu, M.R. Kano, T. Yamori, et al., Improving Drug Potency and Efficacy by Nanocarrier-Mediated Subcellular Targeting, *Sci. Transl. Med.* 3 (2011) 64ra2-64ra2. doi:10.1126/scitranslmed.3001385.
- [16] R. Vivek, R. Thangam, V. Nipunbabu, T. Ponraj, S. Kannan, Oxaliplatin-chitosan nanoparticles induced intrinsic apoptotic signaling pathway: a “smart” drug delivery system to breast cancer cell therapy, *Int. J. Biol. Macromol.* 65 (2014) 289–297. doi:10.1016/j.ijbiomac.2014.01.054.
- [17] Study of MBP-426 in Patients With Second Line Gastric, Gastroesophageal, or Esophageal Adenocarcinoma, <https://ClinicalTrials.gov/Show/NCT00964080>. (n.d.).
- [18] P. Sood, K. Bruce Thurmond, J.E. Jacob, L.K. Waller, G.O. Silva, D.R. Stewart, et al., Synthesis and characterization of AP5346, a novel polymer-linked diaminocyclohexyl platinum chemotherapeutic agent, *Bioconjug. Chem.* 17 (2006) 1270–1279. doi:10.1021/bc0600517.
- [19] J.R. Rice, J.L. Gerberich, D.P. Nowotnik, S.B. Howell, Preclinical Efficacy and Pharmacokinetics of AP5346, A Novel Diaminocyclohexane-Platinum Tumor-Targeting Drug Delivery System, *Clin. Cancer Res.* 12 (2006) 2248 LP – 2254. doi:10.1158/1078-0432.CCR-05-2169.
- [20] H. Cabral, Y. Matsumoto, K. Mizuno, Q. Chen, M. Murakami, M. Kimura, et al., Accumulation of sub-100 nm polymeric micelles in poorly permeable tumours depends on size, *Nat. Nanotechnol.* 6 (2011) 815–823. doi:10.1038/nnano.2011.166.
- [21] H. Cabral, K. Kataoka, Progress of drug-loaded polymeric micelles into clinical studies, *J. Control. Release.* 190 (2014) 465–476. doi:10.1016/j.jconrel.2014.06.042.
- [22] G. Lollo, J.-P. Benoit, M. Brachet, Drug delivery system, European Patent Office 854 (EP18306201.7), 2018.
- [23] F.A. Oyarzun-Ampuero, F.M. Goycoolea, D. Torres, M.J. Alonso, A new drug nanocarrier consisting of polyarginine and hyaluronic acid, *Eur. J. Pharm. Biopharm.* 79 (2011) 54–57. doi:10.1016/j.ejpb.2011.04.008.
- [24] G. Kogan, L. Šoltés, R. Stern, P. Gemeiner, Hyaluronic acid: A natural biopolymer with a broad range of biomedical and industrial applications, *Biotechnol. Lett.* 29 (2007) 17–25. doi:10.1007/s10529-006-9219-z.
- [25] L.C. Becker, W.F. Bergfeld, D. V. Belsito, C.D. Klaassen, J.G. Marks, R.C. Shank, et al., Final Report of the Safety Assessment of Hyaluronic Acid, Potassium Hyaluronate, and Sodium Hyaluronate, *Int. J. Toxicol.* 28 (2009) 5–67. doi:10.1177/1091581809337738.
- [26] N.M. Salwowska, K.A. Bebenek, D.A. Żądło, D.L. Weisło-Dziadecka, Physicochemical properties and application of hyaluronic acid: a systematic review, *J. Cosmet. Dermatol.* 15 (2016) 520–526. doi:10.1111/jocd.12237.
- [27] S. Ganesh, A.K. Iyer, D. V. Morrissey, M.M. Amiji, Hyaluronic acid based self-assembling nanosystems for CD44 target mediated siRNA delivery to solid tumors, *Biomaterials.* 34 (2013) 3489–3502. doi:10.1016/j.biomaterials.2013.01.077.
- [28] S. Ganesh, A.K. Iyer, F. Gattacceca, D. V Morrissey, M.M. Amiji, In vivo biodistribution of siRNA and cisplatin administered using CD44-targeted hyaluronic acid nanoparticles, *J. Control. Release.* 172 (2013) 699–706. doi:https://doi.org/10.1016/j.jconrel.2013.10.016.
- [29] F.A. Oyarzun-Ampuero, F.M. Goycoolea, D. Torres, M.J. Alonso, A new drug nanocarrier consisting of polyarginine and hyaluronic acid, *Eur. J. Pharm. Biopharm. Off. J. Arbeitsgemeinschaft Für Pharm. Verfahrenstechnik e.V.* 79 (2011) 54–57. doi:10.1016/j.ejpb.2011.04.008.
- [30] H. Cabral, N. Nishiyama, K. Kataoka, Optimization of (1,2-diamino-cyclohexane)platinum(II)-loaded polymeric micelles directed to improved tumor targeting and enhanced antitumor activity, *J. Control. Release.* 121 (2007) 146–155. doi:10.1016/j.jconrel.2007.05.024.
- [31] G.R. Dakwar, E. Zagato, J. Delanghe, S. Hobel, A. Aigner, H. Denys, et al., Colloidal stability of nano-sized particles in the peritoneal fluid: Towards optimizing drug delivery systems for intraperitoneal therapy, *Acta Biomater.* 10 (2014) 2965–2975. doi:10.1016/j.actbio.2014.03.012.
- [32] K. Braeckmans, K. Buyens, W. Bouquet, C. Vervaet, P. Joye, F. De Vos, et al., Sizing nanomatter in biological fluids by fluorescence single particle tracking, *Nano Lett.* 10 (2010) 4435–4442. doi:10.1021/nl103264u.
- [33] M. Weyland, A. Griveau, J. Bejaud, J.P. Benoit, P. Coursaget, E. Garcion, Lipid nanocapsule functionalization by lipopeptides derived from human papillomavirus type-16 capsid for nucleic acid delivery into cancer cells, *Int. J. Pharm.* 454 (2013) 756–764. doi:10.1016/j.ijpharm.2013.06.013.
- [34] G. Lollo, M. Vincent, G. Ullio-Gamboa, L. Lemaire, F. Franconi, D. Couez, et al., Development of multifunctional lipid nanocapsules for the co-delivery of paclitaxel and CpG-ODN in the treatment of glioblastoma., *Int. J. Pharm.* 495 (2015) 972–980. doi:10.1016/j.ijpharm.2015.09.062.
- [35] J. Lehner, C. Wittwer, D. Fersching, B. Siegele, O.J. Stotzer, S. Holdenrieder, Methodological and preclinical evaluation of an HMGB1 immunoassay, *Anticancer Res.* 31 (2011) 1989. <http://www.embase.com/search/results?subaction=viewrecord&from=export&id=L70437581>.
- [36] I. Martins, Y. Wang, M. Michaud, Y. Ma, A.Q.

- Sukkurwala, S. Shen, et al., Molecular mechanisms of ATP secretion during immunogenic cell death, *Cell Death Differ.* 21 (2014) 79–91. doi:10.1038/cdd.2013.75.
- [37] P. Marmiroli, B. Riva, E. Pozzi, E. Ballarini, D. Lim, A. Chiorazzi, et al., Susceptibility of different mouse strains to oxaliplatin peripheral neurotoxicity: Phenotypic and genotypic insights, *PLoS One.* 12 (2017) 1–25. doi:10.1371/journal.pone.0186250.
- [38] F. Carton, Y. Chevalier, L. Nicoletti, M. Tarnowska, B. Stella, S. Arpicco, et al., Rationally designed hyaluronic acid-based nano-complexes for pentamidine delivery., *Int. J. Pharm.* 568 (2019) 118526. doi:10.1016/j.ijpharm.2019.118526.
- [39] USP <785>, Osmolality and osmolarity. Available at: [Http://www.Pharmacopeia.cn/v29240/usp29nf24s0_c785.html](http://www.Pharmacopeia.cn/v29240/usp29nf24s0_c785.html), (n.d.).
- [40] N.S. Basakran, CD44 as a potential diagnostic tumor marker, *Saudi Med. J.* 36 (2015) 273–279. doi:10.15537/smj.2015.3.9622.
- [41] J.M. Song, J. Im, R.S. Nho, Y.H. Han, P. Upadhyaya, F. Kassie, Hyaluronan-CD44/RHAMM interaction-dependent cell proliferation and survival in lung cancer cells, *Mol. Carcinog.* 58 (2019) 321–333. doi:10.1002/mc.22930.
- [42] X. Zhao, K. Yang, R. Zhao, T. Ji, X. Wang, X. Yang, et al., Inducing enhanced immunogenic cell death with nanocarrier-based drug delivery systems for pancreatic cancer therapy, *Biomaterials.* 102 (2016) 187–197. doi:10.1016/j.biomaterials.2016.06.032.
- [43] B.A. Cisterna, N. Kamaly, W. Il Choi, A. Tavakkoli, O.C. Farokhzad, C. Vilos, Targeted nanoparticles for colorectal cancer, *Nanomedicine.* 11 (2016) 2443–2456. doi:10.2217/nmm-2016-0194.
- [44] G. Vilar, J. Tulla-Puche, F. Albericio, Polymers and drug delivery systems., *Curr. Drug Deliv.* 9 (2012) 367–94. <http://www.ncbi.nlm.nih.gov/pubmed/22640038>.
- [45] S.P. Atkinson, Z. Andreu, M.J. Vicent, Polymer therapeutics: Biomarkers and new approaches for personalized cancer treatment, *J. Pers. Med.* 8 (2018). doi:10.3390/jpm8010006.
- [46] A. Poveda, R. Salazar, J.M. del Campo, C. Mendiola, J. Cassinello, B. Ojeda, et al., Update in the management of ovarian and cervical carcinoma, *Clin. Transl. Oncol.* 9 (2007) 443–451. doi:10.1007/s12094-007-0083-7.
- [47] M. Creixell, N.A. Peppas, Co-delivery of siRNA and therapeutic agents using nanocarriers to overcome cancer resistance, *Nano Today.* 7 (2012) 367–379. doi:10.1016/j.nantod.2012.06.013.
- [48] H.I. Tsai, L. Jiang, X. Zeng, H. Chen, Z. Li, W. Cheng, et al., DACHPt-loaded nanoparticles self-assembled from biodegradable dendritic copolymer polyglutamic acid-b-D- α -tocopheryl polyethylene glycol 1000 succinate for multidrug resistant lung cancer therapy, *Front. Pharmacol.* 9 (2018) 1–10. doi:10.3389/fphar.2018.00119.
- [49] G. Liu, H. Gao, Y. Zuo, X. Zeng, W. Tao, H. Tsai, et al., DACHPt-Loaded Unimolecular Micelles Based on Hydrophilic Dendritic Block Copolymers for Enhanced Therapy of Lung Cancer, *ACS Appl. Mater. Interfaces.* 9 (2017) 112–119. doi:10.1021/acsami.6b11917.
- [50] B.P. Toole, Hyaluronan and its binding proteins, the hyaladherins, *Curr. Opin. Cell Biol.* 2 (1990) 839–844. doi:[https://doi.org/10.1016/0955-0674\(90\)90081-O](https://doi.org/10.1016/0955-0674(90)90081-O).
- [51] A. Spadea, J.M. Rios De La Rosa, A. Tirella, M.B. Ashford, K.J. Williams, I.J. Stratford, et al., Evaluating the Efficiency of Hyaluronic Acid for Tumor Targeting via CD44, *Mol. Pharm.* 16 (2019) 2481–2493. doi:10.1021/acs.molpharmaceut.9b00083.
- [52] E. Dalla Pozza, C. Lerda, C. Costanzo, M. Donadelli, I. Dando, E. Zoratti, et al., Targeting gemcitabine containing liposomes to CD44 expressing pancreatic adenocarcinoma cells causes an increase in the antitumoral activity, *Biochim. Biophys. Acta - Biomembr.* 1828 (2013) 1396–1404. doi:10.1016/j.bbamem.2013.01.020.
- [53] A.D. Garg, S. More, N. Rufo, O. Mece, M.L. Sassano, P. Agostinis, et al., Trial watch: Immunogenic cell death induction by anticancer chemotherapeutics, *Oncoimmunology.* 6 (2017) e1386829–e1386829. doi:10.1080/2162402X.2017.1386829.
- [54] G. Kroemer, L. Galluzzi, O. Kepp, L. Zitvogel, Immunogenic Cell Death in Cancer Therapy, *Annu. Rev. Immunol.* 31 (2013) 51–72. doi:10.1146/annurev-immunol-032712-100008.
- [55] A.D. Garg, A.M. Dudek-Peric, E. Romano, P. Agostinis, Immunogenic cell death, *Int. J. Dev. Biol.* 59 (2015) 131–140. doi:10.1387/ijdb.150061pa.
- [56] M.A. Graham, G.F. Lockwood, D. Greenslade, S. Brienza, M. Bayssas, E. Gamelin, Clinical Pharmacokinetics of Oxaliplatin: A Critical Review Clinical, *Clin. Cancer Res.* 18 (2000) 1205–1218.
- [57] S. Li, L. Huang, Pharmacokinetics and biodistribution of nanoparticles., *Mol. Pharm.* 5 (2008) 496–504. doi:10.1021/mp800049w.

Supplementary data

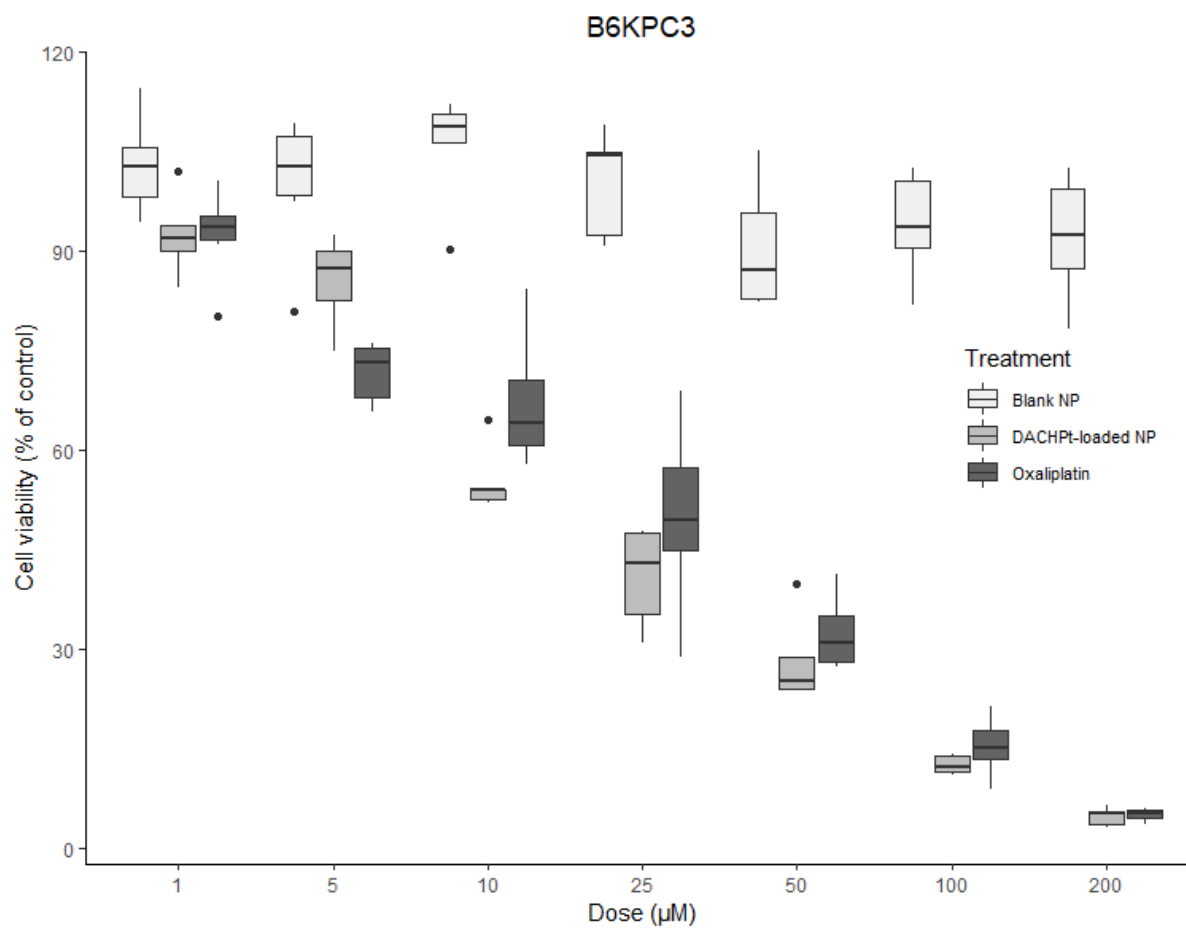


Figure 1 - Viability assessment performed on B6KPC3 cells after 24h of incubation at 37°C with increasing concentrations (0 - 200 μM) of oxaliplatin, blank NP and DACHPt-loaded NP for 24h (n=6).